Enzymatic Properties and Subcellular Localization of Arabidopsis β-*N*-Acetylhexosaminidases[1][W][OA]

Richard Strasser*, Jayakumar Singh Bondili, Jennifer Schoberer, Barbara Svoboda, Eva Liebminger, Josef Glössl, Friedrich Altmann, Herta Steinkellner, and Lukas Mach

Institute of Applied Genetics and Cell Biology (R.S., J.S., B.S., E.L., J.G., H.S., L.M.) and Department of Chemistry (J.S.B., F.A.), BOKU-University of Natural Resources and Applied Life Sciences, A–1190 Vienna, Austria

Plant glycoproteins contain substantial amounts of paucimannosidic *N*-glycans lacking terminal GlcNAc residues at their nonreducing ends. It has been proposed that this is due to the action of β-hexosaminidases during late stages of *N*-glycan processing or in the course of *N*-glycan turnover. We have now cloned the three putative β-hexosaminidase sequences present in the Arabidopsis (*Arabidopsis thaliana*) genome. When heterologously expressed as soluble forms in *Spodoptera frugiperda* cells, the enzymes (termed HEXO1–3) could all hydrolyze the synthetic substrates *p*-nitrophenyl-2-acetamido-2-deoxy-β-D-glucopyranoside, *p*-nitrophenyl-2-acetamido-2-deoxy-β-D-galactopyranoside, 4-methylumbelliferyl-2-acetamido-2-deoxy-β-D-glucopyranoside, and 4-methylumbelliferyl-6-sulfo-2-acetamido-2-deoxy-β-D-glucopyranoside, albeit to a varying extent. HEXO1 to HEXO3 were further able to degrade pyridylaminated chitotriose, whereas pyridylaminated chitobiose was only cleaved by HEXO1. With *N*-glycan substrates, HEXO1 displayed a much higher specific activity than HEXO2 and HEXO3. Nevertheless, all three enzymes were capable of removing terminal GlcNAc residues from the α1,3- and α1,6-mannosyl branches of biantennary *N*-glycans without any strict branch preference. Subcellular localization studies with HEXO-fluorescent protein fusions transiently expressed in *Nicotiana benthamiana* plants showed that HEXO1 is a vacuolar protein. In contrast, HEXO2 and HEXO3 are mainly located at the plasma membrane. These results indicate that HEXO1 participates in *N*-glycan trimming in the vacuole, whereas HEXO2 and/or HEXO3 could be responsible for the processing of *N*-glycans present on secretory glycoproteins.

Most plant glycoproteins contain substantial amounts of paucimannosidic *N*-glycans. These truncated oligosaccharides consist of a pentasaccharide core structure modified with β1,2-linked Xyl and core α1,3-linked Fuc moieties, but lack terminal GlcNAc residues (Lerouge et al., 1998; Wilson et al., 2001). However, substrate specificity analyses of plant *N*-glycan modifying enzymes have revealed that enzymes like Golgi α-mannosidase II (Strasser et al., 2006), β1,2-*N*-acetylglucosaminyltransferase II (Strasser et al., 1999b), β1,2-xylosyltransferase (Bencúr et al., 2005), and core α1,3-fucosyltransferase (Leiter et al., 1999) strictly require the presence of the terminal GlcNAc residue (GlcNAc-1) added by β1,2-*N*-acetylglucosaminyltransferase I to the α1,3-mannosyl branch of *N*-glycans (Strasser et al., 1999a). This strongly indicates that paucimannosidic *N*-glycans are generated by the removal of GlcNAc-1 and its counterpart on the α1,6-linked mannosyl branch (GlcNAc-2) in the final stages of the *N*-glycosylation pathway. Such a removal of terminal GlcNAc residues might take place in the secretory pathway due to the action of a processing β-*N*-acetylglucosaminidase as it has been proposed for insects (Altmann et al., 1995; Léonard et al., 2006). The occurrence of a similar enzyme in plants could be responsible for the presence of paucimannosidic *N*-glycans on extracellular glycoproteins (Takahashi et al., 1986; Sturm, 1991; Fitchette-Lainé et al., 1997) and on recombinant glycoproteins targeted to the apoplast (Cabanes-Macheteau et al., 1999; Dirnberger et al., 2001). Alternatively, terminal GlcNAc residues could be cleaved off either during the transport to or after arrival in the vacuole (Vitale and Chrispeels, 1984; Vitale et al., 1984; Sturm et al., 1987). These observations indicate that GlcNAc trimming constitutes a regular and deliberate event in glycoprotein maturation in plants. However, up to now the enzymes involved in this process have not been identified.

In contrast to the well studied insect, fungal, and mammalian β-*N*-acetylglucosaminidases only limited information is available on the corresponding plant enzymes, although β-hexosaminidases have been detected in a variety of plant tissues, e.g. in seeds, leaves, and suspension cultured cells (Li and Li, 1970; Boller and Kende, 1979; Barber and Ride, 1989; Oikawa et al.,

[1] This work was supported by a grant from the Austrian Science Fund (grant no. P19092 to R.S.) and a PhD studentship from the European Union "Pharma-Planta" project (to J.B.).

* Corresponding author; e-mail richard.strasser@boku.ac.at.

The author responsible for distribution of materials integral to the findings presented in this article in accordance with the policy described in the Instructions for Authors (www.plantphysiol.org) is: Richard Strasser (richard.strasser@boku.ac.at).

[W] The online version of this article contains Web-only data.

[OA] Open Access articles can be viewed online without a subscription.

www.plantphysiol.org/cgi/doi/10.1104/pp.107.101162

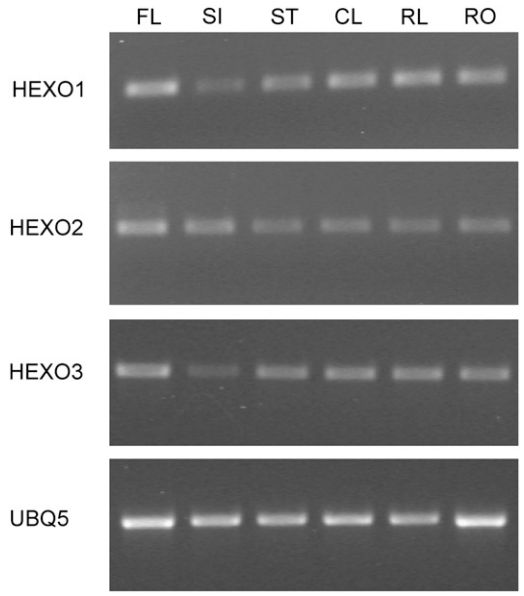

Figure 1. Expression analysis of HEXO1, HEXO2, and HEXO3 mRNA by RT-PCR. RT-PCR was performed with specific primer sets for HEXO1 (31 cycles), HEXO2 (31 cycles), HEXO3 (31 cycles), or UBQ5 as control (35 cycles). FL, Flowers; SI, siliques; ST, stems; CL, cauline leaves; RL, rosette leaves; RO, 12-d-old seedling roots. Each RT-PCR reaction was performed twice with similar results.

2003). In particular, high levels of β-*N*-acetylhexosaminidase activity have been detected in germinating seeds (Bouquelet and Spik, 1978; Yi, 1981; Oikawa et al., 2003), suggesting a physiological role in the metabolism of storage glycoproteins (Harris and Chrispeels, 1975). A function in defense-related processes has also been proposed since several of the purified β-*N*-acetylhexosaminidases could degrade chitin oligomers (Li and Li, 1970; Yi, 1981; Oikawa et al., 2003). However, no plant β-hexosaminidase has yet been characterized on the molecular level.

We have now cloned cDNAs encoding all three candidate β-hexosaminidases (HEXO1–3) identified in the Arabidopsis (*Arabidopsis thaliana*) genome and expressed them heterologously in insect cells. The enzymatic properties of the three proteins were characterized, including a comprehensive assessment of their capacity to act on *N*-glycan substrates. Furthermore, the subcellular localization of the three Arabidopsis β-hexosaminidases was studied in planta.

RESULTS

Identification and Cloning of Arabidopsis β-*N*-Acetylglucosaminidases

To identify Arabidopsis sequences coding for putative β-*N*-acetylglucosaminidases a TBLASTN search in The Arabidopsis Information Resource database (http://www.arabidopsis.org/; dataset: Arabidopsis Genome Initiative Transcripts) was performed using the *Drosophila* β-*N*-acetylglucosaminidase amino acid sequence encoded by the fused lobes gene (FDL; GenBank accession number NM_165909) as an input. Three Arabidopsis homologs (HEXO1: Gene ID At3g55260; HEXO2: Gene ID At1g05590; and HEXO3: Gene ID At1g65590) were found, which have all been assigned to glycoside hydrolase family 20 (β-hexosaminidases: EC 3.2.1.52) in the carbohydrate-active enzymes database (Henrissat and Bairoch, 1993).

To determine whether all three HEXO genes are expressed in Arabidopsis tissues reverse transcription (RT)-PCR was performed using RNA extracted from siliques, flowers, stems, leaves, and roots. Transcripts of the three genes could be detected in all analyzed organs in similar amounts (Fig. 1). All three open reading frames (ORFs) were subsequently amplified by RT-PCR from total RNA isolated from rosette leaves. The RT-PCR products were of the expected size and DNA sequencing revealed no differences between the PCR products and the sequences deposited in the database. HEXO1 ORF (identical to NM_115384) is 1,626 bp long and encodes a protein of 541 amino acids, with a calculated molecular mass of 61.2 kD. The deduced HEXO1 amino acid sequence contains six putative *N*-glycosylation sites (Supplemental Fig. S1). A pairwise sequence alignment using BLASTP (National Center for Biotechnology Information) revealed 31% identity to *Drosophila* FDL, 34% identity to the α-subunit (HEXA, NP_000511) of human lysosomal β-hexosaminidase A, and 34% identity to the β-subunit of the latter enzyme (HEXB, NP_000512). The HEXO2 ORF (1,743 bp, identical to NM_100439) encodes a protein of 580 amino acids, with a molecular mass of 65.0 kD and five potential *N*-glycosylation sites. HEXO2 displays 33% identity to FDL, 32% identity to human HEXA, and 34% identity to human HEXB. The HEXO3 ORF (1,608 bp, identical to NM_105233) encodes a protein of 535 amino acids with a molecular mass of 60.0 kD and five potential *N*-glycosylation sites. Sequence comparisons detected significant identities between HEXO3 and FDL (32%), HEXA (39%), and HEXB (36%). A comparison of HEXO1 and HEXO3 reveals 51% identity, whereas HEXO2 displays only 31% identity to HEXO1 and 29% identity to HEXO3.

In silico topology analysis of the Arabidopsis HEXO proteins suggests that HEXO2 and HEXO3 are type II membrane proteins, with a short N-terminal cytosolic region of six and seven amino acids, respectively, a single transmembrane domain, and a large extracellular/lumenal domain containing the putative catalytic domain (Supplemental Table S1). In contrast, HEXO1 is predicted to lack a transmembrane domain. SignalP analysis revealed that all three proteins probably contain a signal peptide for translocation into the lumen of the endoplasmic reticulum. However, the predicted signal anchor and cleavage site probabilities are rather low for all three HEXO proteins.

An alignment of Arabidopsis HEXO proteins, human HEXA, human HEXB, and *Drosophila* FDL is

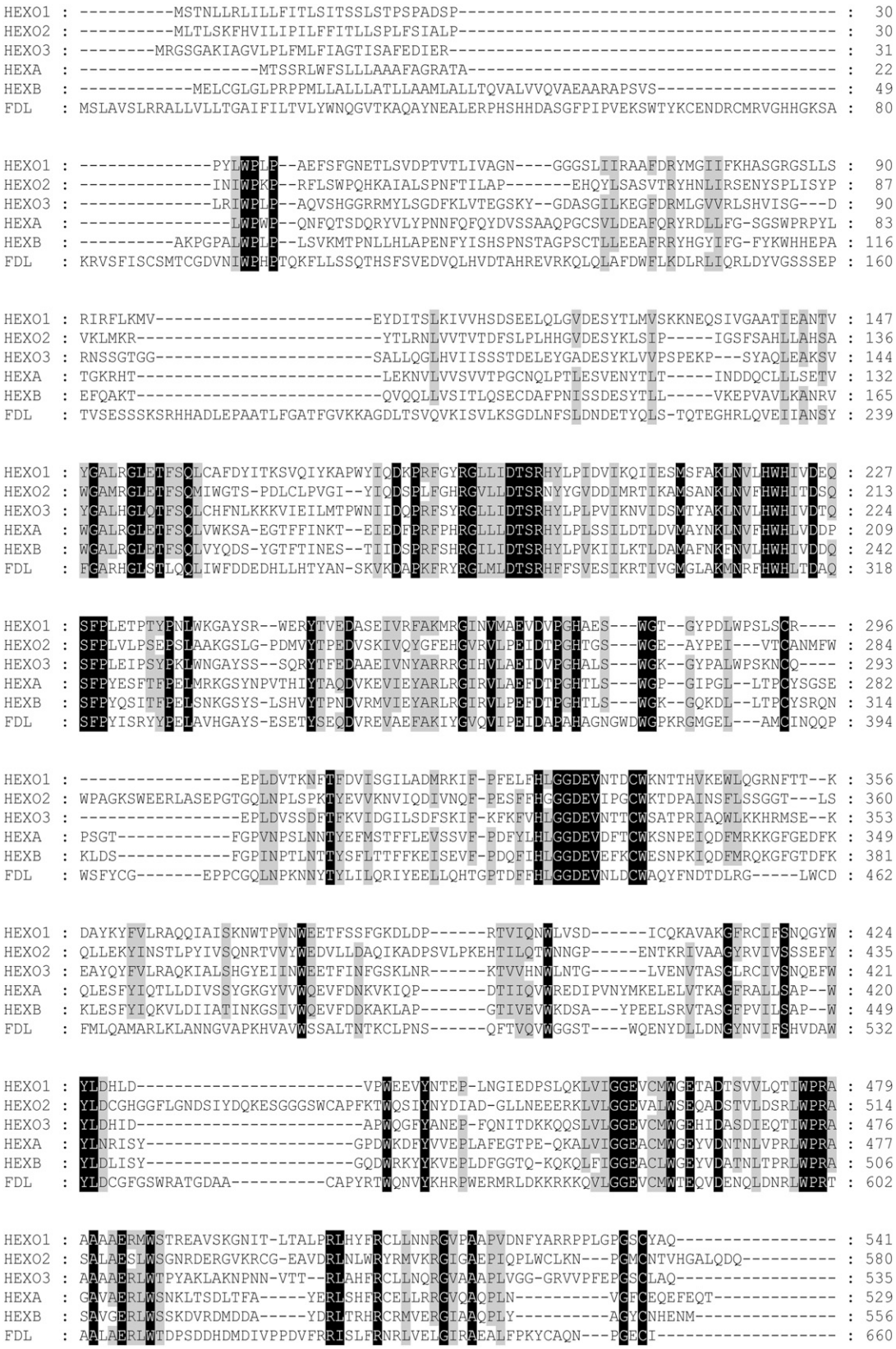

Figure 2. Multiple sequence alignment of HEXO and *Drosophila* FDL proteins with human hexosaminidases A and B. The sequence alignment was performed with ClustalW and was edited manually. Conserved amino acid residues are shaded black

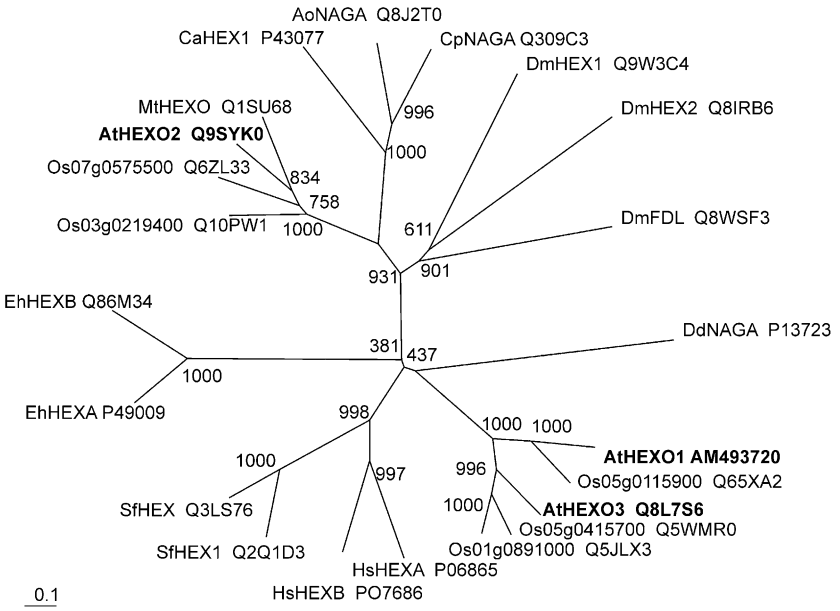

Figure 3. Cladogram showing the relationship of selected β-hexosaminidases from glycoside hydrolase family 20. Values at branch nodes indicate numbers of bootstrap trials out of 1,000 that produced each node. The 0.1 scale represents 10% change. Sequences: Ao, *Aspergillus oryzae*; At, Arabidopsis; Ca, *Candida albicans*; Cp, *Coccidioides posadasii*; Dd, *Dictyostelium discoideum*; Dm, *Drosophila melanogaster*; Eh, *Entamoeba histolytica*; Hs, *Homo sapiens*; Mt, *Medicago truncatula*; Os, *Oryzae sativa*; Sf, *Spodoptera frugiperda*. UniProt and EMBL database accession numbers of the proteins are shown.

shown in Figure 2. Comparison with the crystal structure of human lysosomal β-hexosaminidase A (Lemieux et al., 2006) shows that residues involved in substrate binding (R211, D354, Y450, D452, and E491; HEXB numbering) and the formation of the catalytic triad (D240, H294, E355) are conserved in all three Arabidopsis HEXO proteins. Furthermore, HEXA and HEXB residues for which missense mutations have been identified are almost completely conserved in all three HEXOs (Lemieux et al., 2006). R424 from HEXA, which has been found to be implicated in binding of negatively charged substrates (Sharma et al., 2003), is not present in any of the HEXO sequences. The conserved Cys residues C309, C360, and C551 engaged in disulfide bridges are present in all three HEXO sequences. C534, which forms a disulfide bond with C551 in HEXA and HEXB is found in HEXO1 and HEXO3, but not in HEXO2.

A phylogenetic analysis was performed using selected β-hexosaminidase sequences from glycoside hydrolase family 20 (Fig. 3). The analysis revealed that HEXO2 is distinct from HEXO1 and HEXO3 and closely related to fungal β-hexosaminidases, whereas HEXO1 and HEXO3 rather resemble the human lysosomal β-hexosaminidase subunits. Five putative β-hexosaminidase sequences homologous to the three HEXO proteins could be found in the rice (*Oryza sativa*) genome. One putative rice β-hexosaminidase (UniProt database identifier Q65XA2) is 66% identical to HEXO1, whereas HEXO2 shows 56% identity to two other rice proteins (Q6ZL33 and Q10PW1) probably representing paralogs. HEXO3 has an identity of 63% to two rice proteins (Q5WMR0 and Q5JLX3) assigned to glycoside hydrolase family 20. The latter two rice amino acid sequences differ only modestly (73% identity) and thus might also represent paralogs.

Heterologous Expression of Arabidopsis HEXO Proteins in Insect Cells

Production of HEXO proteins was achieved in *S. frugiperda* Sf21 cells by means of baculovirus mediated expression. For this purpose the putative catalytic domain of HEXO1 lacking its 32 N-terminal amino acids was cloned into baculovirus transfer vector pVTBac-His-1 (Sarkar et al., 1998). HEXO2 and HEXO3 lacking their 32 and 29 N-terminal amino acids, respectively, were also expressed as soluble forms in Sf21 cells. Immunoblot analysis of cell extracts and culture supernatants revealed that all three proteins were successfully expressed in Sf21 cells and secreted into the culture medium (data not shown).

Biochemical Characterization of the Recombinant Arabidopsis HEXO Proteins

The secreted recombinant proteins were purified from culture supernatants of HEXO-producing Sf21 cells by means of nickel-chelate affinity chromatography.

Figure 2. (*Continued.*)
and similar residues are depicted in gray. Dashed lines represent gaps inserted for optimal alignment of the sequences. HEXO1, Arabidopsis HEXO1; HEXO2, Arabidopsis HEXO2; HEXO3, Arabidopsis HEXO3; FDL, *Drosophila* FDL protein; HEXA, human hexosaminidase A; HEXB, human hexosaminidase B.

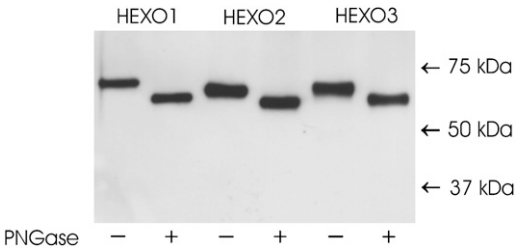

Figure 4. Western blot of heterologously expressed HEXO enzymes. Purified recombinant HEXO proteins were incubated overnight in the absence (−) or presence (+) of PNGase F, analyzed by SDS-PAGE under reducing conditions, and subjected to western-blot analysis with anti-His antibodies.

Immunoblot analysis with antibodies to the His tag of the purified fusion proteins revealed major immunoreactive bands of 68 (HEXO1), 64 (HEXO2), and 65 kD (HEXO3; Fig. 4). The detected sizes of the recombinant polypeptides were in close agreement with their theoretical molecular masses, considering that the proteins contain five to six potential *N*-glycosylation sites. Peptide *N*-glycosidase F (PNGase F) digestion led to 62, 60, and 61 kD bands, respectively, which shows that all three recombinant polypeptides are *N*-glycosylated. For deglycosylated HEXO1 and HEXO3 the detected molecular masses correspond very well to the calculated ones (61.8 and 61.0 kD). The calculated molecular mass of deglycosylated HEXO2 is 65.6 kD, which is higher than the observed molecular mass of the recombinant fusion protein. To rule out that the expressed HEXO2 transcript is incomplete, e.g. due to a cryptic splice site, HEXO2 cDNA was amplified from RNA extracted from baculovirus-infected cells and sequenced. No changes to the original HEXO2 sequence were found, indicating that the transcript expressed in the infected cells codes for a full-length HEXO2 protein. Since His antibodies directed against the N-terminal fusion tag (Fig. 4) and antibodies against a C-terminal HEXO2 peptide (data not shown) reacted with purified recombinant HEXO2, we conclude that recombinant HEXO2 displays an anomalous migration behavior in SDS-PAGE gels.

Purified recombinant HEXO proteins were assayed using different synthetic substrates (*p*-nitrophenyl-2-acetamido-2-deoxy-β-D-glucopyranoside [*p*NP-GlcNAc], *p*-nitrophenyl-2-acetamido-2-deoxy-β-D-galactopyranoside [*p*NP-GalNAc], 4-methylumbelliferyl-2-acetamido-2-deoxy-β-D-glucopyranoside [MU-GlcNAc], MU-GlcNAc-6SO_4). In addition to the heterologously expressed Arabidopsis proteins, the assays were also performed with a commercially available β-hexosaminidase purified from jack bean (*Canavalia ensiformis*) meal (Li and Li, 1970). For all three HEXO proteins *p*NP-GlcNAc was the preferred substrate over *p*NP-GalNAc as also observed for the jack bean enzyme (Table I).

All three purified HEXO proteins were also active on the fluorogenic MU-GlcNAc substrate. For HEXO1 and jack bean β-hexosaminidase the specific activities for *p*NP-GlcNAc and MU-GlcNAc were almost identical, while for HEXO2 and HEXO3 the MU-GlcNAc activity was 2- to 3-fold lower at the given substrate concentrations. Its sulfated derivative (MU-GlcNAc-6SO_4) was also hydrolyzed by all three Arabidopsis enzymes, albeit with much lower efficiency. HEXO2 hydrolyzed MU-GlcNAc-6SO_4 similarly poorly as HEXO1, whereas the sulfate group particularly strongly interferes with hydrolysis by HEXO3.

The pH optima for *p*NP-GlcNAc hydrolysis was 4.0 for HEXO1 and 5.0 for HEXO2, HEXO3, and jack bean β-hexosaminidase (Fig. 5A). The apparent K_m and V_{max} values for *p*NP-GlcNAc were found to be 0.7 mM and 151 μmol min^{-1} mg^{-1} for HEXO1, 1.2 mM and 7.9 μmol min^{-1} mg^{-1} for HEXO2, 2.2 mM and 50.3 μmol min^{-1} mg^{-1} for HEXO3, and 1.9 mM and 31.1 μmol min^{-1} mg^{-1} for jack bean β-hexosaminidase. These K_m and V_{max} values are in the same range as reported for other plant β-hexosaminidases (Li and Li, 1970; Barber and Ride, 1989; Jin et al., 2002).

To address the question whether complex *N*-glycans are substrates for the three Arabidopsis β-hexosaminidases, pyridylaminated-GnGn (GnGn-PA; for structural details see Supplemental Fig. S2) and other *N*-glycan substrates were analyzed (Table II). The PA-oligosaccharide substrates were incubated with purified recombinant HEXO proteins and the reaction products were analyzed by reverse-phase HPLC. With the GnGn-PA substrate, release of GlcNAc was clearly detected for

Table I. *Activity of HEXO proteins and jack bean β-hexosaminidase (Sigma) with synthetic substrates*

Activities were determined at substrate concentrations of 5 mM (*p*NP substrates) or 1 mM (MU substrates) in 50 mM sodium citrate buffer (pH 4.6) at 37°C.

Substrate	Enzyme Protein (HEXO) or Total Protein (Jack Bean)			
	HEXO1	HEXO2	HEXO3	Jack Bean
	μmol min⁻¹ mg⁻¹			
*p*NP-GlcNAc	132	6.35	34.9	22.5
*p*NP-GalNAc	9.35	2.48	3.63	13.9
MU-GlcNAc	151	2.26	11.2	23.0
MU-GlcNAc-6SO_4	0.283	0.222	0.008	0.068

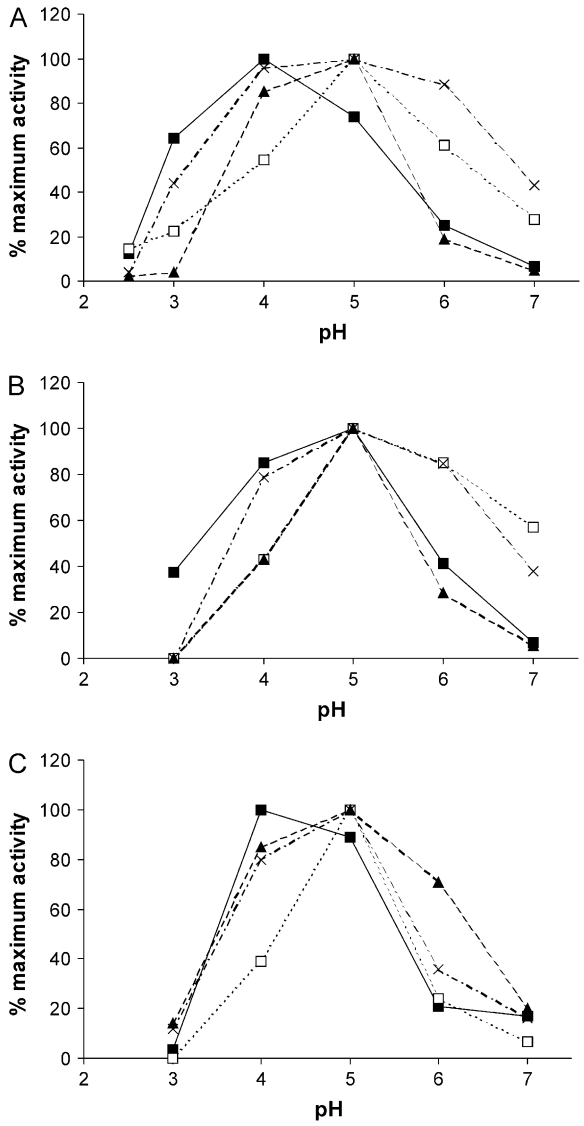

Figure 5. Influence of pH on the activity of recombinant HEXO enzymes. The ability of HEXO1 (■), HEXO2 (□), HEXO3 (▲), and jack bean β-hexosaminidase (x) to hydrolyze *p*NP-GlcNAc (A), GnGn-PA (B), and $(GlcNAc)_3$-PA (C) was analyzed under different pH conditions.

all three HEXO proteins. However, the rate of GlcNAc release varied considerably between the three enzymes. HEXO1 displayed a much higher specific activity than HEXO2 and HEXO3. The incubation of HEXO1 and HEXO3 with GnGn-PA resulted in the formation of three product peaks (GnM-, MGn-, and MM-PA; Fig. 6A; Table II). Incubation with HEXO2 resulted in the formation of GnM-PA and MGn-PA while MM-PA was not detectable. Although the enzymes do not show a strict selectivity for either GlcNAc-1 or GlcNAc-2, the main reaction product was GnM-PA. In comparison with the other Arabidopsis enzymes HEXO1 showed the most pronounced preference for the hydrolysis of GlcNAc-1 from GnGn-PA (i.e. yielding GnM-PA), whereas jack bean β-hexosaminidase displayed only a modest preference.

To determine the substrate specificity in more detail enzyme assays were performed with GnM-PA and MGn-PA substrates, which both contain a single nonreducing terminal GlcNAc residue attached either to the α1,6-mannosyl (GnM-PA) or α1,3-mannosyl (MGn-PA) branch of the *N*-glycan core. In contrast to the recently characterized *Drosophila* FDL enzyme, which specifically cleaves MGn-PA (Léonard et al., 2006), all three HEXO proteins hydrolyzed both substrates. The specific activity of HEXO1 with GnM-PA was 2-fold higher than with MGn-PA. In contrast to that HEXO2 and HEXO3 displayed preferential hydrolysis of MGn-PA (Table II). These results demonstrate that HEXO2 can also generate MM-PA. The failure of the enzyme to produce detectable amounts of MM-PA in the GnGn-PA assays is most likely due to the generally rather low activity of HEXO2 with *N*-glycan substrates (Table II).

Man5Gn-PA is not hydrolyzed by *Drosophila* FDL, but was cleaved by the Arabidopsis HEXO proteins as well as jack bean β-hexosaminidase. All Arabidopsis enzymes were capable of cleaving off GlcNAc residues from both branches of the physiologically most relevant *N*-glycan substrate GnGnXF-PA (Fig. 6B; Table II), which contains the β1,2-linked Xyl and core α1,3-linked Fuc residues typical for plant *N*-glycans. Importantly, presence of the latter residues does not influence the rate of GlcNAc liberation significantly. Assays with jack bean β-hexosaminidase gave results comparable to those obtained for the Arabidopsis HEXO enzymes. The pH optima of the enzymes for hydrolysis of *N*-glycan substrates were determined using GnGn-PA and found to be 5.0 for all four plant β-*N*-acetylglucosaminidases tested (Fig. 5B).

HEXO activity toward two labeled chitooligosaccharides, GlcNAcβ1,4GlcNAcβ1,4GlcNAc-PA [$(GlcNAc)_3$-PA] and GlcNAcβ1,4GlcNAc-PA [$(GlcNAc)_2$-PA], was also analyzed. $(GlcNAc)_3$-PA was hydrolyzed to $(GlcNAc)_2$-PA by jack bean β-hexosaminidase and by all three HEXO enzymes, although the specific activity of HEXO3 was quite low (Table II). HEXO2 displayed, in comparison to HEXO3, a high specific activity with $(GlcNAc)_3$-PA. Assays performed with $(GlcNAc)_2$-PA as substrate revealed efficient hydrolysis of this compound by HEXO1 and jack bean β-hexosaminidase. For HEXO2 and HEXO3 $(GlcNAc)_2$-PA hydrolysis was not detectable. The pH optimum for $(GlcNAc)_3$-PA hydrolysis was 4.0 for HEXO1 and pH 5.0 for the other three enzymes (Fig. 5C).

Subcellular Localization of HEXO Proteins

Substrate specificity analyses of the recombinant HEXOs clearly demonstrate that all three proteins process *N*-glycans. To obtain a better understanding about the individual functional roles of the three HEXO proteins during *N*-glycan biosynthesis, their

Table II. *Activity of HEXO proteins and jack bean β-hexosaminidase (Sigma) with N-glycan and chitooligosaccharide substrates*

Substrate (5 μM) was incubated with HEXO and jack bean enzymes in 0.1 M sodium citrate/phosphate buffer (pH 5.0) for different times at 30°C. The samples were then analyzed by reverse-phase HPLC. For GnGn-PA and GnGnXF-PA, the hydrolysis rates shown are derived from assays where less than 5% of the substrate was converted into MM-PA or MMXF-PA, respectively.

Substrate	Products	Enzyme Protein (HEXO) or Total Protein (Jack Bean)			
		HEXO1	HEXO2	HEXO3	Jack Bean
		pmol min^{-1} mg^{-1}			
GnGn-PA	GnM-PA	3.2×10^4	5.4	37.8	1.8×10^3
GnGn-PA	MGn-PA	2.6×10^3	0.7	9.8	1.2×10^3
MGn-PA	MM-PA	3.2×10^3	3.0	33.0	410
GnM-PA	MM-PA	6.4×10^3	1.0	22.0	620
GnGnXF-PA	GnMXF-PA	4.4×10^4	3.8	40.2	1.0×10^3
GnGnXF-PA	MGnXF-PA	1.6×10^3	0.8	7.0	700
Man5Gn-PA	Man5-PA	3.0×10^3	4.1	21.6	800
$(GlcNAc)_3$-PA	$(GlcNAc)_2$-PA	3.0×10^3	1.2×10^3	27.5	1.0×10^3
$(GlcNAc)_2$-PA	GlcNAc-PA	1.0×10^3	<2	<1	400

subcellular location was analyzed in planta. To this end GFP was fused to the C terminus of the HEXO proteins and the fusion proteins were transiently expressed in *Nicotiana benthamiana* leaf epidermal cells. Confocal laser-scanning microscopy revealed that HEXO2-GFP and HEXO3-GFP were localized exclusively at the extreme cell periphery and clearly labeled the outline of the cells (Fig. 7, A and D), indicating targeting to the plasma membrane. No Golgi or vacuolar labeling could be observed for these two fusion proteins. To reveal the organelle identity, labeling of the cells with a well established plasma membrane marker (FM4-64) was performed (Batoko et al., 2000). A clear colocalization of FM4-64 with HEXO3 (Fig. 7, A–C) and HEXO2 was obtained (Fig. 7, D–F), which provides further evidence for plasma membrane targeting of the two enzymes. Additionally we wanted to investigate whether the two HEXO enzymes colocalize with a plasma membrane protein fused to GFP (EGFP-LTI6b; Kurup et al., 2005). To colocalize HEXO3 with EGFP-LTI6b it was necessary to replace GFP by cyan fluorescent protein (CFP). As shown in Figure 7G HEXO3-CFP accumulated like HEXO3-GFP at the cell periphery and colocalized with EGFP-LTI6b (Fig. 7, G–I). Coexpression of HEXO2-GFP with HEXO3-CFP revealed again a distinct colocalization (Fig. 7, J–L), indicating that HEXO2 and HEXO3 are targeted to the same destination, the plasma membrane.

In contrast to HEXO3-GFP and HEXO2-GFP, HEXO1-GFP displayed a faint but uniform fluorescence pattern across the whole cell (Supplemental Fig. S3). This HEXO1-GFP signal indicated targeting to the large central vacuole that occupies almost the whole cell, since the vacuolar marker construct aleu-GFP (Humair et al., 2001) showed a similar subcellular distribution, while cytosolic GFP clearly displayed a different labeling behavior with nuclei and cytoplasmic strands also being stained (Supplemental Fig. S3). For colocalization experiments with aleu-GFP, an additional HEXO1 construct with a carboxy-terminal monomeric red fluorescent protein (mRFP) moiety was generated. HEXO1-mRFP clearly displayed a fluorescence pattern reminiscent of a vacuolar protein, as demonstrated by colocalization with aleu-GFP (Fig. 7, M–O). This strongly indicates the presence of HEXO1 in the central vacuole of transfected *N. benthamiana* leaf epidermal cells.

DISCUSSION

The initial steps during *N*-glycan biosynthesis in plants are well characterized (Bencúr et al., 2005; Gomord et al., 2005; Strasser et al., 2006). It is well documented that the addition of a GlcNAc residue to the $Man_5GlcNAc_2$ core structure by β1,2-*N*-acetylglucosaminyltransferase I initiates the formation of complex and paucimannosidic *N*-glycans. Processing enzymes that act further downstream in the pathway strictly require the presence of this terminal β1,2-linked GlcNAc on the α1,3-Man branch (see Supplemental Fig. S4). However, very little is known about the conversion of complex into paucimannosidic oligosaccharides and the formation of the Lewis a epitope, which is the only known outer chain elongation found in complex plant *N*-glycans. It has been suggested that the biosynthesis of the Lewis a epitope occurs in the trans part of the Golgi apparatus (Fitchette et al., 1999). In contrast, the subcellular compartments accounting for the formation of paucimannosidic *N*-glycans have not yet been identified.

Paucimannosidic structures can be found in wild-type plants as well as in various Arabidopsis mutants with defects in the plant *N*-glycan processing pathway (Strasser et al., 2004, 2006). Based on our in vitro studies HEXO1 appears to be the most relevant enzyme for their generation since it shows a much higher hydrolysis rate of *N*-glycan substrates than the other HEXOs.

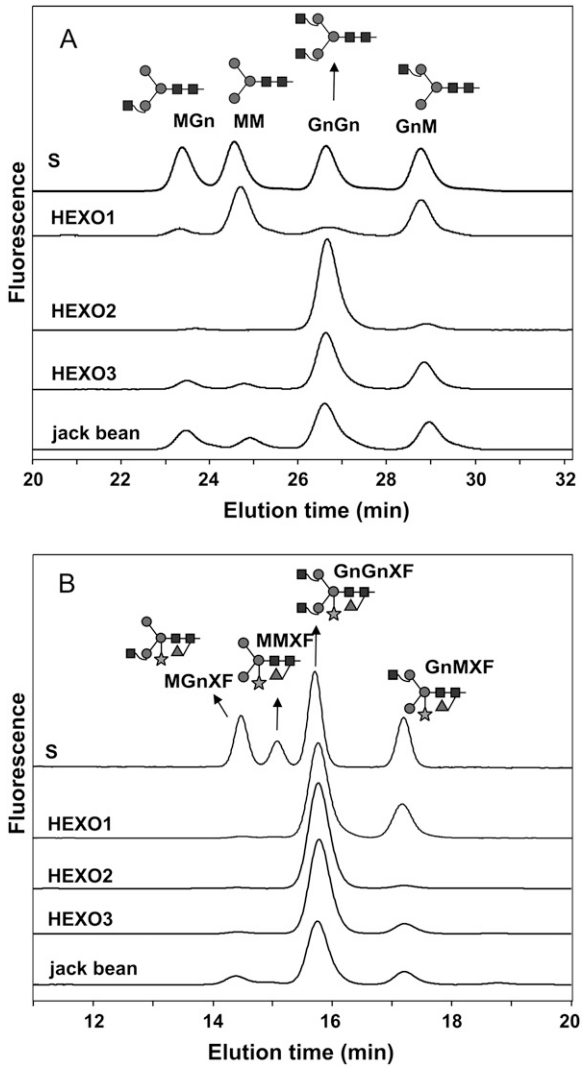

Figure 6. Activity assays of recombinant HEXO enzymes and jack bean β-hexosaminidase with GnGn-PA (A) and GnGnXF-PA (B) as substrates. The samples were analyzed by reverse-phase HPLC with fluorescence detection. PA oligosaccharides were incubated with either 30 ng of purified HEXO1, 1.3 μg of HEXO2, 1.6 μg of HEXO3, and 300 ng of jack bean β-hexosaminidase. The reactions were stopped after 1 h (HEXO1 and jack bean β-hexosaminidase) or 16 h (HEXO2 and HEXO3) of incubation. The elution positions of standards (MGn-, MM-, GnGn-, GnM-PA and MGnXF-, MMXF-, GnGnXF-, GnMXF-PA) are shown (S).

However, all three HEXO proteins appear capable of generating these structures in vivo. Furthermore, we clearly show that all Arabidopsis HEXOs have no strict preference for the hydrolysis of GlcNAc-1 or GlcNAc-2 and are thus different from *Drosophila* FDL, which removes exclusively the GlcNAc-1 residue (Léonard et al., 2006).

The enzymatic properties of HEXO1 to HEXO3 were found to be comparable to those of jack bean β-hexosaminidase with respect to substrate specificity, pH optima, and K_m values. In the case of *N*-glycan substrates, the jack bean enzyme displayed similar properties as HEXO1. It has been already previously reported that jack bean β-hexosaminidase is capable of releasing GlcNAc residues from glycoprotein substrates (Li and Li, 1970). Moreover, analysis of tryptic peptides of jack bean β-hexosaminidase by liquid chromatography/electrospray ionization-mass spectrometry revealed sequences homologous to HEXO1 (J. Stadlmann, F. Altmann, and R. Strasser, unpublished data), indicating that these two enzymes are indeed closely related.

The occurrence of several related β-hexosaminidases has been also described for other plant species. For example, four β-hexosaminidase isoforms have been isolated from germinating seeds of fenugreek (Bouquelet and Spik, 1978). These isoenzymes display subtle differences in their M_r, K_m values toward synthetic substrates, pH optima, and substrate specificities. Interestingly, the enzymatic properties of the three Arabidopsis HEXOs are in a similar range. While most of the plant β-hexosaminidases studied to date were analyzed for their activity toward synthetic substrates and chitin oligomers, the ability to liberate GlcNAc residues from *N*-glycan substrates was only tested for a limited number of enzymes. A β-hexosaminidase isolated from cotton (*Gossypium hirsutum*) seedlings was found to release GlcNAc residues from glycoprotein substrates (Yi, 1981). However, only two of the four isoforms from fenugreek were able to remove β1,2-linked GlcNAc residues from *N*-glycans (Bouquelet and Spik, 1978), while the purified β-*N*-acetylhexosaminidase from maize (*Zea mays*) seedlings displayed no detectable activity with *N*-glycan and glycoprotein substrates (Oikawa et al., 2003).

The subcellular localization data obtained with the fluorescent HEXO fusion proteins are in good agreement with proteomic analyses of plant organelles. HEXO1 was identified in the vegetative vacuole proteome of Arabidopsis (Carter et al., 2004) and in the tonoplast fraction of Arabidopsis suspension cells (Shimaoka et al., 2004), but was not detected within the proteome of integral membrane proteins of the tonoplast (Szponarski et al., 2004). In contrast to that HEXO2 was neither identified in these nor in any other proteomic studies reported so far. However, our analysis of HEXO2 mRNA expression indicates that HEXO2 transcripts are detectable in various plant tissues without any significant organ-specific variation, suggesting that the HEXO2 gene is ubiquitously expressed. HEXO3 was detected recently in the apoplastic fluid of Arabidopsis rosette leaves (Boudart et al., 2005). Since none of the HEXOs has been localized in the Golgi apparatus it seems that the removal of GlcNAc residues from nascent *N*-glycans does not take place in this subcellular compartment as suggested for insect cells (Altmann et al., 1995).

The differences in their subcellular localization and activities indicate that the three HEXOs are involved in

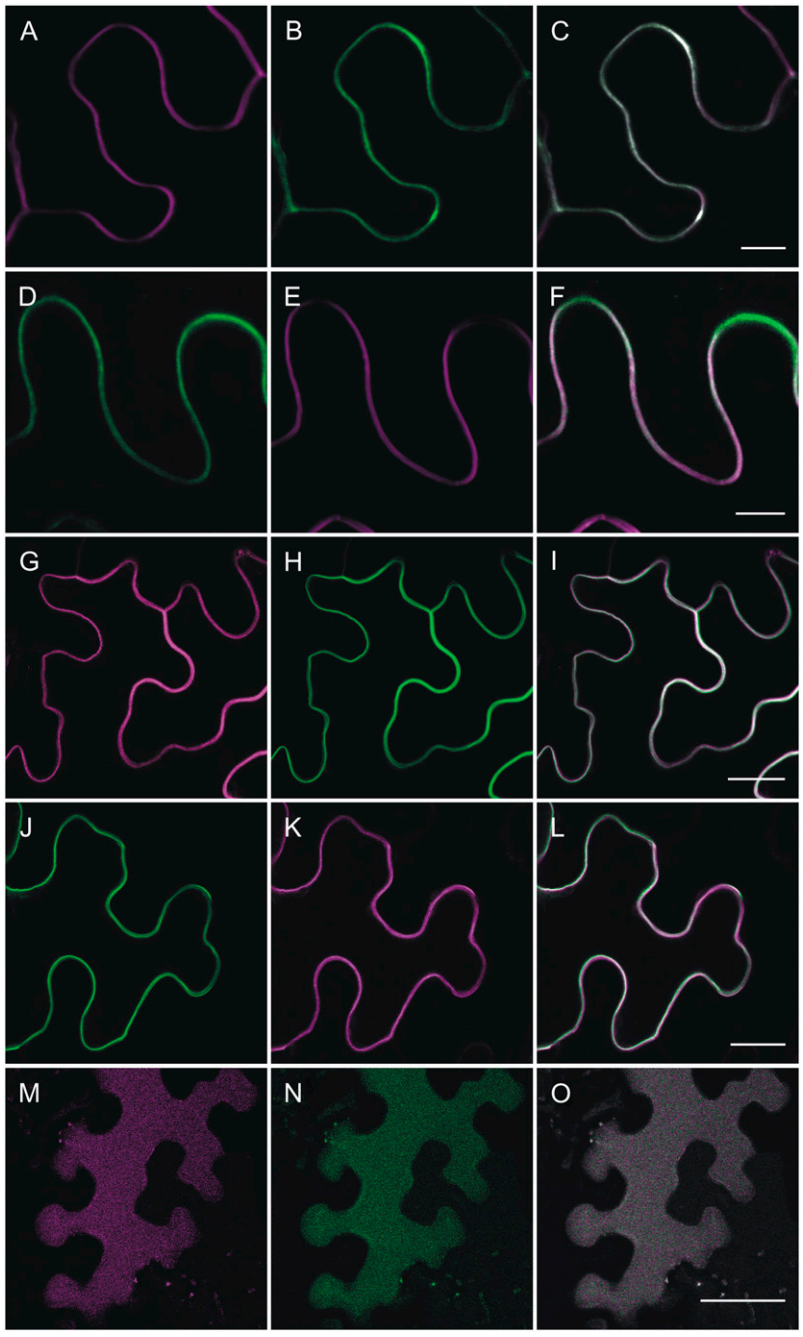

Figure 7. Expression of fluorescent HEXO fusion constructs in *N. benthamiana* leaf epidermal cells. A, Transient expression of HEXO2-GFP. B, FM4-64 labeling of the plasma membrane. C, Overlay of images A and B, scale bar = 10 μm. D, Expression of HEXO3-GFP. E, FM4-64 staining of the plasma membrane. F, Overlay of images D and E, scale bar = 10 μm. G, Expression of HEXO3-CFP. H, Expression of plasma membrane marker EGFP-LTI6b. I, Overlay of images G and H, scale bar = 20 μm. J, Expression of HEXO2-GFP. K, Expression of HEXO3-CFP. L, Overlay of images K and L, scale bar = 20 μm. M, Expression of HEXO1-mRFP. N, Expression of aleu-GFP. O, Overlay of images M and N, scale bar = 50 μm.

different cellular processes. The comparatively high specific activity of HEXO1 toward *N*-glycan substrates, together with its acidic pH optimum suggests that HEXO1 is involved in the generation of the MMXF structures typically found on vacuolar glycoproteins and thus has mainly a catabolic role. This conclusion is consistent with its subcellular location in the vacuole.

As HEXO2 and HEXO3 have been localized at the plasma membrane they could act on *N*-glycans from plasma membrane proteins and on secreted glycoproteins. However, due to their relatively low activity with *N*-glycan substrates as compared to HEXO1, they might have additional functions. In particular, HEXO2, which has the lowest activity toward *N*-glycans, efficiently releases GlcNAc residues from chitotriose and thus could be involved in plant defense reactions, like chitin-elicited lignification. This has been previously suggested for other plant β-hexosaminidases (Barber and Ride, 1989). However, additional experiments are required to define the exact physiological functions of the individual Arabidopsis HEXO proteins.

MATERIALS AND METHODS

Homology Search and Phylogenetic Analysis

Amino acids were aligned using ClustalW (http://www.ddbj.nig.ac.jp/search/clustalw-e.html). The phylogenetic analysis was done using the neighbor-joining method with bootstrapping analysis (1,000 replicates) and the cladogram was graphically displayed using TreeView software (http://taxonomy.zoology.gla.ac.uk/rod/treeview.html).

RT-PCR and Cloning of Arabidopsis HEXO cDNAs

Total RNA was purified from organs of Arabidopsis wild-type (Columbia-0) plants using a SV Total RNA Isolation kit (Promega). Semiquantitative RT-PCR was performed using primers for ubiquitin (control) UBQ5-D 5′-AACCCTTGAGGTTGAATCATC-3′ and UBQ5-F 5′-CTCCTTCTTTCTGGTAAACGT-3′, and the following HEXO-specific primers: HEXO1: At3g55260-4F 5′-GTATAATCTTTAAACACGCTTCTGGTAG-3′/At3g55260-6R 5′-GGCTAAATGTCTCCAATCCTCTAAGT-3′, HEXO2: At1g05590-1 5′-TATTAAGGCCATGAGTGCAAACAAAC-3′/At1g05590-3 5′-GCTAACCGCTCTTCCCAACTTTT-3′, and HEXO3: At1g65590-4F 5′-AAAATGAGAGGTAGCGGAGCAAAGAT-3′/At1g65590-7R 5′-AAAATGAGAGGTAGCGGAGCAAAGAT-3′. The HEXO1 coding region was amplified with Taq-Polymerase (Peqlab) from cDNA using the forward primer At3g55260-5F 5′-CGAAAATGTCAACGAATCTTCTTC-3′ and the reverse primer At3g55260-8R 5′-TCACTGAGCATAGCAAGAGCCAGG-3′ and subcloned into pGEM-T vector (Promega). The HEXO2 and HEXO3 ORFs were amplified with ULTRA Pfu-Polymerase (Stratagene) using primers At1g05590-4F 5′-AGAACAAGTCATGCTAACTCTTTCCAAGT-3′ and At1g05590-5R 5′-CTGTTTTTATTGATCTTGAAGAGCACCA-3′ and primers At1g65590-4F 5′-AAAATGAGAGGTAGCGGAGCAAAGAT-3′ and At1g65590-5R 5′-GAATCACTGAGCGAGACAAGAACCTG-3′, respectively, and subcloned using a Zero Blunt Topo PCR Cloning kit (Invitrogen). Individual clones from all three amplified coding sequences were sequenced using the PRISM BigDye Terminator Cycle Sequencing kit and an ABI 3100 genetic analyzer (Applied Biosystems).

Expression in Insect Cells

The N-terminal deletion construct of HEXO1 containing amino acids 33 to 541 was generated by PCR using primers AtHex1-Xba-F 5′-TATATCTAGACTATGGCCGTTACCGGCGGAGT-3′ and AtHex1-Not-R 5′-TATAGCGGCCGCATCACTGAGCATAGCAAGAGCCA-3′. The PCR product was cleaved with *Xba*I and *Not*I restriction enzymes at the underlined sites and ligated into pVTBac-His-1 baculovirus transfer vector (Sarkar et al., 1998), digested with the same enzymes. In this construct, the truncated HEXO protein is placed downstream of the melittin signal peptide, a 6xHis tag, and an enterokinase cleavage sequence. Fragments encoding N-terminally truncated versions of HEXO2 (amino acids 33–580) and HEXO3 (amino acids 30–535) were generated and subcloned as above using primers AtHex2-Pst-F 5′-TATACTGCAGATTTGGCCAAAGCCGAGATTTCT-3′ and AtHex2-Kpn-R 5′-TATAGGTACCTTATTGATCTTGAAGAGCACCAT-3′ (HEXO2) and primers AtHex3-Xba-R 5′-TATATCTAGAGAGAGGTTGAGGATTTGGC-3′ and AtHex3-Not-R 5′-AATAGCGGCCGCATCACTGAGCGAGACAAGAACCTGG-3′ (HEXO3). Expression in *Spodoptera frugiperda* Sf21 cells, purification, and quantification of recombinant HEXO proteins as well as enzymatic deglycosylation using PNGase F (Roche) was performed essentially as described previously (Bencúr et al., 2005). Immunoblot detection of the recombinant HEXO forms was done using anti-His antibodies (CLONTECH) or antibodies recognizing the enterokinase cleavage sequence (Invitrogen).

Assays with Synthetic Substrates

Assays with *p*NP substrates were performed in a total volume of 40 μL of assay buffer (50 mM sodium citrate buffer [pH 4.6], 1 mg mL^{-1} bovine serum albumin, 0.02% [w/v] NaN_3) containing either 5 mM *p*NP-GlcNAc or *p*NP-GalNAc (both from Sigma). After incubation at 37°C for an appropriate time, the reactions were stopped by addition of 80 μL of 0.4 M Gly buffer (pH 10.4) prior to spectrophotometric analysis at 405 nm. Assays with MU substrates were performed in a total volume of 200 μL of assay buffer containing either 1 mM MU-GlcNAc (Sigma) or 4-methylumbelliferyl-6-sulfo-2-acetamido-2-deoxy-β-D-glucopyranoside (Calbiochem). After incubation at 37°C for an appropriate time, the reactions were stopped by addition of 1 mL of 0.4 M Gly buffer (pH 10.4) prior to spectrofluorimetry using excitation and emission wavelengths of 365 nm and 460 nm, respectively. Sodium citrate/phosphate buffers (0.1 M; pH 2.5–7.0) were used for assay of the pH dependency of the enzymes for hydrolysis of *p*NP-GlcNAc. K_m values were deduced from Hanes-Woolf plots of the data at 12 different concentrations of *p*NP-GlcNAc ranging from 0.1 mM to 6 mM. The values represent the means of three independent experiments.

Assays with PA Substrates

PA oligosaccharide substrates GnGn-PA, GnM-PA, and MGn-PA were prepared as previously described (Altmann et al., 1995). Man5Gn-PA was prepared from Man5-PA by incubation with recombinant tobacco (*Nicotiana tabacum*) β1,2-*N*-acetylglucosaminyltransferase I (Strasser et al., 1999a). GnGnXF-PA was purified from PA-labeled asparagus (*Asparagus officinalis*) glycans by reverse-phase HPLC (Wilson et al., 2001). $(GlcNAc)_3$-PA and $(GlcNAc)_2$-PA were available from previous studies (Léonard et al., 2006). Assays with PA oligosaccharides were performed in a total volume of 20 μL of 0.1 M sodium citrate/phosphate buffer (pH 5.0) containing 5 μM substrate. After incubation at 30°C for an appropriate time, the reactions were stopped by addition of 80 μL of 20 mM sodium borate. Aliquots of 50 μL were analyzed by reverse-phase HPLC as previously described (Léonard et al., 2006). Sodium citrate/phosphate buffers (0.1 M; pH 3.0–7.0) were used for assay of the pH dependency of the enzymes for hydrolysis of GnGn-PA and $(GlcNAc)_3$-PA.

Translational HEXO-Fluorescent Protein Fusions

To generate carboxy-terminal fusion proteins the HEXO1 coding region lacking the stop codon was amplified by PCR using forward primer At3g55260-9F 5′-TATATCTAGAAAATGTCAACGAATCTTCTTC-3′ and reverse primer At3g55260-10R 5′-TATATCTAGACTGAGCATAGCAAGAGCCAGG-3′ and subcloned into the *Xba*I site of binary plant transformation vector p20F to generate p20F-HEXO1. For the construction of p20F, PCR-amplified enhanced GFP cDNA (kindly provided by Christian Luschnig, our institute) lacking the start codon was inserted into the *Bam*HI site of plant expression vector pPT2 (Strasser et al., 2005), thus placing expression of the fusion constructs under the control of the cauliflower mosaic virus 35S promoter. Vector p20F-HEXO2 (HEXO2-GFP) was generated by inserting the HEXO2 PCR product obtained with primers AtHex2-Xba-F 5′-TTTTTCTAGAAATGCTAACTCTTTCCAAGTTTCA-3′ and AtHex2-Bgl-R 5′-AATTAGATCTTTGATCTTGAAGAGCACCAT-3′ into *Xba*I/*Bam*HI digested p20F. The HEXO3 ORF was amplified with primer AtHex3-Xba-F2 5′-TATATCTAGAAAATGAGAGGTAGCGGAGCAAAG-3′ and AtHex3-Xba-R 5′-TATATCTAGACTGAGCGAGACAAGAACC-3′ and cloned into the *Xba*I site of p20F to generate p20F-HEXO3 (HEXO3-GFP). The mRFP-vector pPFH3L is derived from pPFH2 (M. Schähs, H. Steinkellner, and R. Strasser, unpublished data), a derivative of pPT2. The mRFP cDNA, kindly provided by Roger Y. Tsien (University of California, San Diego), was amplified using forward primer mRFP3 5′-TATAGGTACCATGGCCTCCTCCGAGGACGTC-3′ and reverse primer mRFP2 5′-TATAGGATCCTTAGGCGCCGGTGGAGTGG-3′ and ligated into *Kpn*I/*Bam*HI digested vector pPFH2 to create pPFH3. A small linker fragment was generated by annealing the two primers mRFPL1 5′-CTAGAGCTGGAAATGGTGCAGGTAC-3′ and mRFPL2 5′-CTGCACCATTTCCAGCT-3′ and ligated into *Xba*I/*Kpn*I digested pPFH3, which resulted in vector pPFH3L. To generate the HEXO1-mRFP fusion construct the HEXO1 coding sequence from p20F-HEXO1 was released using *Xba*I, gel purified, and ligated into *Xba*I digested pPFH3L vector. To construct HEXO3-CFP, the HEXO3 coding sequence was released from HEXO3-GFP using *Xba*I and ligated into *Xba*I digested vector p23. Vector p23 was generated by PCR amplification of the CFP coding region of CFP cDNA (kindly provided by Chris Hawes, Oxford Brookes University) with the forward primer CFP-1 (5′-TATAGGATCCGGAGGTGGAGGTGTGAGCAAGGGCGAGGAGCTGTTC-3′) and the reverse primer CFP-2 (5′-TATAAGATCTTTACTTGTACAGCTCGTCCATG-3′). The PCR product was cleaved with *Bam*HI/*Bgl*II and ligated into *Bam*HI digested vector pPT2. The sequences of all fusion constructs were confirmed by DNA sequencing.

Plant Material and *Agrobacterium*-Mediated Transient Expression

Nicotiana benthamiana plants were grown in a growth chamber at 22°C with a 16-h light/8-h dark photoperiod. Five- to 6-week-old plants were used for agroinfiltration experiments following the protocol of Batoko et al. (2000). Briefly, HEXO fusion constructs were transformed into *Agrobacterium tumefaciens* strains UIA143 or GV3101 (pMP90) by electroporation. A single colony

arising from each transformation was inoculated into 5 mL Luria-Bertani medium supplemented with 50 μg mL^{-1} kanamycin and 25 μg mL^{-1} gentamycin and grown to stationary phase (20–24 h) at 29°C with agitation. Three-hundred microliters of bacterial culture was centrifuged and washed twice with infiltration buffer (50 mM MES, pH 5.6, 2 mM sodium phosphate, 0.5% [w/v] D-Glc, and 100 μM acetosyringone). For plant infiltration, resuspended bacteria were diluted to an OD_{600} of 0.3 for HEXO1-mRFP, 0.01 for aleu-GFP, and 0.1 for EGFP-LTI6b, HEXO2-GFP, HEXO3-GFP, and HEXO3-CFP. For experiments requiring coexpression of two different constructs, appropriate volumes of each bacterial suspension were mixed prior to infiltration. Diluted bacterial suspensions were injected through the stomata on the lower epidermal surface of fully expanded leaves using a 1 mL plastic syringe and gentle pressure. Infiltrated plants were returned to the growth chamber. Fluorescent protein expression was analyzed in lower epidermal cells 2, 3, and 4 d postinfiltration.

Sampling and Imaging

Small leaf pieces were randomly cut out of the infiltrated area and mounted in water in a way that the abaxial epidermis was facing upwards. Confocal imaging was conducted on a Leica TCS SP2 confocal laser scanning microscope. Images were obtained with a 40× 1.25 numerical aperture or 63× 1.4 numerical aperture oil immersion objective. GFP was imaged using a 488 nm argon laser line and its emission was recorded from 505 to 535 nm, whereas mRFP was excited with a 543 nm HeNe laser line and its emission was collected at 605 to 635 nm. CFP was imaged using a 458 nm argon laser line and its signal was detected at 465 to 495 nm. For FM4-64 staining, fluorescent protein expressing leaf tissue was infiltrated through stomata on the abaxial leaf surface with a solution of 50 μM FM4-64FX (Invitrogen) in distilled water. After 15 min incubation under light at room temperature specimens were examined by confocal microscopy. Dual detection of FM4-64FX and GFP was done with 488-nm argon laser lines and 543-nm HeNe laser lines. GFP-dependent fluorescence was detected at 505 to 535 nm, whereas FM4-64FX staining was recorded at 635 to 680 nm. Postacquisition processing of images was done using Adobe Photoshop CS software.

Supplemental Data

The following materials are available in the online version of this article.

Supplemental Figure S1. Nucleotide and deduced amino acid sequences of Arabidopsis HEXOs.

Supplemental Figure S2. Nomenclature of *N*-glycan structures as used in this study.

Supplemental Figure S3. Subcellular localization of HEXO1-GFP and cytosolic GFP.

Supplemental Figure S4. Late stages of the protein *N*-glycosylation pathway in plants.

Supplemental Table S1. In silico analysis of Arabidopsis HEXO proteins.

ACKNOWLEDGMENTS

We thank Ulrike Vavra and Christiane Veit for expert technical assistance, Thomas Dalik for providing *N*-glycan substrates, and Martin Pabst for assisting with the purification of GnGnXF-PA (all from University of Natural Resources and Applied Life Sciences). We would also like to thank Chris Hawes (Oxford Brookes University) for the kind gift of ST-CFP, John Runions (Oxford Brookes University) for EGFP-LTI6b, and Nadine Paris (Université de Rouen) for the aleu-GFP construct. Sarah Irons (Oxford Brookes University) is gratefully acknowledged for helpful discussions of confocal microscopy data.

Received April 17, 2007; accepted July 10, 2007; published July 20, 2007.

LITERATURE CITED

Altmann F, Schwihla H, Staudacher E, Glössl J, März L (1995) Insect cells contain an unusual, membrane-bound beta-N-acetylglucosaminidase probably involved in the processing of protein N-glycans. J Biol Chem **270:** 17344–17349

Barber MS, Ride JP (1989) Purification and properties of a wheat leaf N-acetyl-b-hexosaminidase. Plant Sci **60:** 163–172

Batoko H, Zheng H, Hawes C, Moore I (2000) A rab1 GTPase is required for transport between the endoplasmic reticulum and golgi apparatus and for normal golgi movement in plants. Plant Cell **12:** 2201–2218

Bencúr P, Steinkellner H, Svoboda B, Mucha J, Strasser R, Kolarich D, Hann S, Köllensperger G, Glössl J, Altmann F, et al (2005) *Arabidopsis thaliana* beta1,2-xylosyltransferase: an unusual glycosyltransferase with the potential to act at multiple stages of the plant N-glycosylation pathway. Biochem J **388:** 515–525

Boller T, Kende H (1979) Hydrolytic enzymes in the central vacuole of plant cells. Plant Physiol **63:** 1123–1132

Boudart G, Jamet E, Rossignol M, Lafitte C, Borderies G, Jauneau A, Esquerré-Tugayé M, Pont-Lezica R (2005) Cell wall proteins in apoplastic fluids of Arabidopsis thaliana rosettes: identification by mass spectrometry and bioinformatics. Proteomics **5:** 212–221

Bouquelet S, Spik G (1978) Properties of four molecular forms of N-acetyl-beta-D-hexosaminidase isolated from germinating seeds of fenugreek (Trigonella foenum graecum). Eur J Biochem **84:** 551–559

Cabanes-Macheteau M, Fitchette-Lainé A, Loutelier-Bourhis C, Lange C, Vine N, Ma J, Lerouge P, Faye L (1999) N-glycosylation of a mouse IgG expressed in transgenic tobacco plants. Glycobiology **9:** 365–372

Carter C, Pan S, Zouhar J, Avila E, Girke T, Raikhel N (2004) The vegetative vacuole proteome of *Arabidopsis thaliana* reveals predicted and unexpected proteins. Plant Cell **16:** 3285–3303

Dirnberger D, Steinkellner H, Abdennebi L, Remy J, van de Wiel D (2001) Secretion of biologically active glycoforms of bovine follicle stimulating hormone in plants. Eur J Biochem **268:** 4570–4579

Fitchette A, Cabanes-Macheteau M, Marvin L, Martin B, Satiat-Jeunemaitre B, Gomord V, Crooks K, Lerouge P, Faye L, Hawes C (1999) Biosynthesis and immunolocalization of Lewis a-containing *N*-glycans in the plant cell. Plant Physiol **121:** 333–344

Fitchette-Lainé A, Gomord V, Cabanes M, Michalski J, Saint Macary M, Foucher B, Cavelier B, Hawes C, Lerouge P, Faye L (1997) N-glycans harboring the Lewis a epitope are expressed at the surface of plant cells. Plant J **12:** 1411–1417

Gomord V, Chamberlain P, Jefferis R, Faye L (2005) Biopharmaceutical production in plants: problems, solutions and opportunities. Trends Biotechnol **23:** 559–565

Harris N, Chrispeels M (1975) Histochemical and biochemical observations on storage protein metabolism and protein body autolysis in cotyledons of germinating mung beans. Plant Physiol **56:** 292–299

Henrissat B, Bairoch A (1993) New families in the classification of glycosyl hydrolases based on amino acid sequence similarities. Biochem J **293:** 781–788

Humair D, Hernández Felipe D, Neuhaus J, Paris N (2001) Demonstration in yeast of the function of BP-80, a putative plant vacuolar sorting receptor. Plant Cell **13:** 781–792

Jin Y, Jo Y, Kim K, Shim J, Kim Y, Park R (2002) Purification and characterization of beta-N-acetylhexosaminidase from rice seeds. J Biochem Mol Biol **35:** 313–319

Kurup S, Runions J, Köhler U, Laplaze L, Hodge S, Haseloff J (2005) Marking cell lineages in living tissues. Plant J **42:** 444–453

Leiter H, Mucha J, Staudacher E, Grimm R, Glössl J, Altmann F (1999) Purification, cDNA cloning, and expression of GDP-L-Fuc:Asn-linked GlcNAc alpha1,3-fucosyltransferase from mung beans. J Biol Chem **274:** 21830–21839

Lemieux M, Mark B, Cherney M, Withers S, Mahuran D, James M (2006) Crystallographic structure of human beta-hexosaminidase A: interpretation of Tay-Sachs mutations and loss of GM2 ganglioside hydrolysis. J Mol Biol **359:** 913–929

Léonard R, Rendic D, Rabouille C, Wilson I, Préat T, Altmann F (2006) The Drosophila fused lobes gene encodes an N-acetylglucosaminidase involved in N-glycan processing. J Biol Chem **281:** 4867–4875

Lerouge P, Cabanes-Macheteau M, Rayon C, Fischette-Lainé A, Gomord V, Faye L (1998) N-glycoprotein biosynthesis in plants: recent developments and future trends. Plant Mol Biol **38:** 31–48

Li S, Li Y (1970) Studies on the glycosidases of jack bean meal. 3. Crystallization and properties of beta-N-acetylhexosaminidase. J Biol Chem **245:** 5153–5160

Oikawa A, Itoh E, Ishihara A, Iwamura H (2003) Purification and characterization of beta-N-acetylhexosaminidase from maize seedlings. J Plant Physiol **160:** 991–999

Sarkar M, Pagny S, Unligil U, Joziasse D, Mucha J, Glössl J, Schachter H (1998) Removal of 106 amino acids from the N-terminus of UDP-GlcNAc: alpha-3-D-mannoside beta-1,2-N-acetylglucosaminyltransferase I does not inactivate the enzyme. Glycoconj J **15:** 193–197

Sharma R, Bukovac S, Callahan J, Mahuran D (2003) A single site in human beta-hexosaminidase A binds both 6-sulfate-groups on hexosamines and the sialic acid moiety of GM2 ganglioside. Biochim Biophys Acta **1637:** 113–118

Shimaoka T, Ohnishi M, Sazuka T, Mitsuhashi N, Hara-Nishimura I, Shimazaki K, Maeshima M, Yokota A, Tomizawa K, Mimura T (2004) Isolation of intact vacuoles and proteomic analysis of tonoplast from suspension-cultured cells of *Arabidopsis thaliana*. Plant Cell Physiol **45:** 672–683

Strasser R, Altmann F, Mach L, Glössl J, Steinkellner H (2004) Generation of *Arabidopsis thaliana* plants with complex N-glycans lacking beta1,2-linked xylose and core alpha1,3-linked fucose. FEBS Lett **561:** 132–136

Strasser R, Mucha J, Schwihla H, Altmann F, Glössl J, Steinkellner H (1999a) Molecular cloning and characterization of cDNA coding for beta1, 2N-acetylglucosaminyltransferase I (GlcNAc-TI) from *Nicotiana tabacum*. Glycobiology **9:** 779–785

Strasser R, Schoberer J, Jin C, Glössl J, Mach L, Steinkellner H (2006) Molecular cloning and characterization of Arabidopsis thaliana Golgi alpha-mannosidase II, a key enzyme in the formation of complex N-glycans in plants. Plant J **45:** 789–803

Strasser R, Stadlmann J, Svoboda B, Altmann F, Glössl J, Mach L (2005) Molecular basis of N-acetylglucosaminyltransferase I deficiency in *Arabidopsis thaliana* plants lacking complex N-glycans. Biochem J **387:** 385–391

Strasser R, Steinkellner H, Borén M, Altmann F, Mach L, Glössl J, Mucha J (1999b) Molecular cloning of cDNA encoding N-acetylglucosaminyltransferase II from *Arabidopsis thaliana*. Glycoconj J **16:** 787–791

Sturm A (1991) Heterogeneity of the complex N-linked oligosaccharides at specific glycosylation sites of two secreted carrot glycoproteins. Eur J Biochem **199:** 169–179

Sturm A, Van Kuik J, Vliegenthart J, Chrispeels M (1987) Structure, position, and biosynthesis of the high mannose and the complex oligosaccharide side chains of the bean storage protein phaseolin. J Biol Chem **262:** 13392–13403

Szponarski W, Sommerer N, Boyer J, Rossignol M, Gibrat R (2004) Large-scale characterization of integral proteins from Arabidopsis vacuolar membrane by two-dimensional liquid chromatography. Proteomics **4:** 397–406

Takahashi N, Hotta T, Ishihara H, Mori M, Tejima S, Bligny R, Akazawa T, Endo S, Arata Y (1986) Xylose-containing common structural unit in N-linked oligosaccharides of laccase from sycamore cells. Biochemistry **25:** 388–395

Vitale A, Chrispeels M (1984) Transient N-acetylglucosamine in the biosynthesis of phytohemagglutinin: attachment in the Golgi apparatus and removal in protein bodies. J Cell Biol **99:** 133–140

Vitale A, Warner TG, Chrispeels MJ (1984) Phaseolus vulgaris phytohemagglutinin contains high-mannose and modified oligosaccharide chains. Planta **160:** 256–263

Wilson I, Zeleny R, Kolarich D, Staudacher E, Stroop C, Kamerling J, Altmann F (2001) Analysis of Asn-linked glycans from vegetable foodstuffs: widespread occurrence of Lewis a, core alpha1,3-linked fucose and xylose substitutions. Glycobiology **11:** 261–274

Yi C (1981) Increase in beta-N-acetylglucosaminidase activity during germination of cotton seeds. Plant Physiol **67:** 68–73